



**HAL**  
open science

## Clearwing butterflies challenge the thermal melanism hypothesis

Violaine Ossola, Fabien Pottier, Charline Pinna, Katia Bougiouri, Aurélie Tournié, Anne Michelin, Christine Andraud, Doris Gomez, Marianne Elias

► **To cite this version:**

Violaine Ossola, Fabien Pottier, Charline Pinna, Katia Bougiouri, Aurélie Tournié, et al.. Clearwing butterflies challenge the thermal melanism hypothesis. 2023. hal-04257566

**HAL Id: hal-04257566**

**<https://hal.science/hal-04257566>**

Preprint submitted on 25 Oct 2023

**HAL** is a multi-disciplinary open access archive for the deposit and dissemination of scientific research documents, whether they are published or not. The documents may come from teaching and research institutions in France or abroad, or from public or private research centers.

L'archive ouverte pluridisciplinaire **HAL**, est destinée au dépôt et à la diffusion de documents scientifiques de niveau recherche, publiés ou non, émanant des établissements d'enseignement et de recherche français ou étrangers, des laboratoires publics ou privés.

1 **Main Manuscript for**

## 2 **Clearwing butterflies challenge the thermal melanism hypothesis**

3

4 **Authors :**

5 Violaine Ossola<sup>1,2</sup>, Fabien Pottier<sup>3</sup>, Charline Pinna<sup>1</sup>, Katia Bougiouri<sup>4</sup>, Aurélie Tournié<sup>3</sup>, Anne  
6 Michelin<sup>3</sup>, Christine Andraud<sup>3\*</sup>, Doris Gomez<sup>4\*</sup>, Marianne Elias<sup>1\*</sup>.

7 \* equal contribution

8

9 **Affiliations:**

10 <sup>1</sup> ISYEB, UMR 7205, CNRS, MNHN, Sorbonne Université, EPHE, France

11 <sup>2</sup> Université Paris Cité, Paris, France

12 <sup>3</sup> CRC, MNHN, Paris, France

13 <sup>4</sup> CEFE, Université of Montpellier, CNRS, EPHE, IRD, Université Paul Valéry Montpellier 3,  
14 Montpellier, France

15 **Corresponding author:** Violaine Ossola

16 [violaine.ossola@gmail.com](mailto:violaine.ossola@gmail.com)

17 Isyeb, 45 rue Buffon, 75005, Paris, France

+33 6 44 75 75 98

18 **Author contributions :** VO, CA, DG, CP and ME designed the study. VO, CA, DG, ME, FP and  
19 CP defined the protocol. ME and DG collected the specimens. VO, CP and FP performed  
20 measurements with the contribution of KB, AT and AM. VO analysed the data. VO, CA, DG, ME  
21 authors wrote the manuscript with contribution of all the authors.

22

23 **Competing Interest Statement:** The authors declare no conflict of interest.

24 **Keywords:** Altitude, Optics, Thermal melanism, Thermal properties, transparency.

25 **This PDF file includes:**

26 Main Text

27 Figures 1 to 4

28

29

30

31 **Abstract**

32

33 In contrast to most butterflies harboring opaque wing colorations, some species display large  
34 transparent patches on their wings. Wing transparency, which entails a dramatic reduction of  
35 pigmentation, raises the question of potential costs for vital functions, such as thermoregulation,  
36 especially along climatic gradients. The thermal melanism hypothesis posits that darker colorations  
37 should be favored in colder environments, which enables them to absorb more radiation and  
38 maintain a body temperature compatible with activity. This prediction extends to the near infrared  
39 (NIR) range, which represents a large proportion of solar radiation. Here we assess the implications  
40 of wing transparency for light absorption and thermal properties in 42 butterfly species from the  
41 neotropical tribe Ithomiini that range the extent of transparency, from fully opaque to highly  
42 transparent, and we test whether those species conform to the prediction of the thermal melanism  
43 hypothesis. We find that transparent wings are less efficient than opaque wings to absorb light  
44 across UV, Visible and NIR wavelength ranges, and are also less efficient to collect heat. Moreover,  
45 dark coloration occupies a lower proportion of wing area as altitude increases, and ithomiine  
46 species harbor more transparency at higher altitudes, where climatic conditions are colder, going  
47 strongly against the prediction of the thermal melanism hypothesis. We discuss these surprising  
48 results in light of recent studies suggesting that factors other than adaptation to cold, such as  
49 predation pressure, physiology or behavior, may have driven the evolution of wing patterns in  
50 Ithomiini.

51

52 **Significance Statement**

53

54 The thermal melanism hypothesis predicts that organisms should be darker and absorb solar  
55 radiation more efficiently in colder environments. The Neotropical butterflies Ithomiini are unusual  
56 in that many species harbor large transparent patches on their wings, raising questions related to  
57 their efficacy of solar radiation absorption and heating capacities. We investigate optical and  
58 thermal properties of several ithomiine species along a climatic gradient. We find that transparent  
59 wings are less efficient at absorbing radiation and collecting heat. Unexpectedly, the proportion of  
60 transparent species increases with altitude, challenging the thermal melanism hypothesis and  
61 suggesting that factors other than adaptation to cold, such as predation pressure, may have driven  
62 the evolution of wing patterns in Ithomiini.

63

64

65

66 **Main Text**

67

68 **Introduction**

69

70 Diurnal butterflies are known for the great variety of colors they display. The scales covering their  
71 wings produce colorations through pigments (1) or structures (2, 3). Coloration is involved in  
72 multiple functions, including intraspecific signaling (4); antipredator defenses such as crypsis and  
73 camouflage (5), masquerade (6), aposematism and mimicry (7); as well as thermal adaptation (8).  
74 The balance between these selective pressures drives the diversity of color patterns in butterfly  
75 wings (9).

76 In ectotherms, coloration has been shown to play an important role in determining body  
77 temperature and activity, since the degree of darkness is positively correlated with internal body  
78 temperature (10). Darker butterfly wings absorb more light, and are associated with longer flight  
79 activity and larger flight distances in cold conditions than lighter wings (11, 12).

80 The thermal melanism hypothesis (TMH) posits that darker colorations provide thermal  
81 advantages in cold environments (13), especially for ectotherms, as dark surfaces are more  
82 efficient to absorb heat from the environment than light surfaces. Darker species or individuals are  
83 expected to live at high altitudes or latitudes, whereas lighter ones are more likely to be present at  
84 lower altitudes and latitudes, which offer warmer conditions. The existence of such melanism  
85 gradients has been shown in many case studies, across geographical regions and wide ranges of  
86 taxa, from reptiles to insects (14–16). However, visible colors represent only a small part of the  
87 incident solar radiation reaching the earth's surface. Over 50% of the solar energy lies in the near-  
88 infrared wavelengths (NIR, 700 to 2500 nm). NIR should then be of particular importance in  
89 ectotherm thermal capacities, more than ultraviolet to red (i. e. 300 to 700 nm, hereafter UV-Visible  
90 range) (17), since they are not involved in other aspects of their ecology because they cannot be  
91 seen by most organisms. Recent studies on communities of European (18) and Australian (19)  
92 butterflies confirmed that reflectance in the NIR range is strongly correlated with climatic factors,  
93 especially temperature, and more strongly compared to UV and Visible wavelengths. In colder  
94 environments, butterflies tend to reflect less and therefore absorb more in the NIR. These findings  
95 highlight that optical properties can be disconnected to a certain extent between NIR and UV-Visible  
96 ranges. By contrast, no clear trends exist regarding humidity or precipitation and wing darkness.  
97 Gloger's rule, which predicts that darker individual should be found in more humid climates, has  
98 been evidenced mainly for endotherms with little clear support in ectotherms (18, 20).

99 In Lepidoptera, few species exhibit transparency on their wings, a feature that has evolved  
100 multiple times independently (21). Transparency is achieved by a large diversity of wing  
101 microstructures, including a combination of scale shape or insertion modification, reduced scale

102 size or density, as well as a reduction of scale pigments (21). In many cases, transparency is  
103 enhanced by the presence of nanostructures on the wing membrane, which decreases reflection  
104 (22–24). Transparency has attracted recent research effort regarding its now-established role in  
105 crypsis in various species (25–27), and its involvement in predator-prey signaling in some clades  
106 of mimetic Lepidoptera (22). Yet, transparency may come at the cost of other functions involving  
107 wing coloration, notably thermoregulation. While thermoregulatory processes are well documented  
108 in opaque species, they are largely unknown in clearwing butterflies. A study focusing on wing  
109 transparency across the entire Lepidoptera order found that clearwing species tend to transmit less  
110 light, and thus absorb more, in high latitudes than in tropical climates, suggesting a thermal cost  
111 for butterflies (21). Yet, the actual impact of transparent wing patches on wing thermal properties  
112 needs to be investigated.

113         Among Lepidoptera, Ithomiini is a remarkable neotropical tribe of ca. 400 species (28, 29),  
114 80% of which exhibit transparency on their wings to some extent. Species are highly segregated  
115 along the elevational gradient, from warm lowlands up to colder highlands, as high as 3,000 meters  
116 (29, 30). Because wing transparency in Ithomiini is achieved by a reduction in membrane coverage  
117 by scales (21, 22), and is therefore associated with a lower quantity of pigments, one might expect  
118 those areas to poorly absorb solar light. Previous studies of geographical distribution of Ithomiini  
119 wing patterns revealed that the proportion of clearwing species increases with altitude, to the extent  
120 that all species above 2000 m have transparent wings (29, 30), contrary to the predictions of the  
121 TMH. Yet, this observation is based on the UV-Visible range (22, 29, 30), and optical transparency  
122 shown in that range may be dissociated from the absorption properties in the NIR.

123         Here, we investigate for the first time wing traits relevant for thermal adaptation in 42  
124 transparent and opaque Ithomiini species that represent the diversity of wing colorations, by using  
125 Infrared imaging and spectrophotometry. We assess the distribution of these wing traits in relation  
126 to the climatic conditions the species are exposed to in a phylogenetic framework. Specifically, we  
127 characterize and quantify the optical and thermal properties of transparent and opaque wing  
128 patches to investigate two mutually exclusive scenarios:

129 (i) *Absorption compensation*: in this scenario, the higher transmission and lower absorption of  
130 wavelengths in the UV-Visible range of transparent wing areas are compensated by a high  
131 absorption in the NIR, and the thermal capacities of transparent wings may be similar to or even  
132 better than those of opaque wings. Under this hypothesis, adaptation to climatic conditions may  
133 drive the altitudinal distribution of wing patterns in Ithomiini.

134 (ii) *Thermal cost*: in this scenario, the disconnection between wavelength ranges is not significant  
135 enough, with transparent wings transmitting more and absorbing less in the NIR range than opaque  
136 wings, therefore, reflecting similar absorption patterns at shorter wavelengths. This results in  
137 transparency being costly in terms of intrinsic heating capacities. Under the thermal cost scenario,

138 thermal properties may not be the main target of selection with regard to the altitudinal distribution  
139 of wing patterns in Ithomiini.

140

141 In addition, assuming that opaque patches - even if not covering a high proportion of the wing  
142 surface in transparent species – may follow the thermal melanism hypothesis, we tested whether  
143 they represent a higher proportion of wing surface in species found in colder climates, a mechanism  
144 that could also compensate for poorer thermal capacities of transparency under the *thermal cost*  
145 scenario. The absence of evidence of compensation mechanisms (disconnection NIR from UV-  
146 Visible range, or increased proportion of opaque patches with altitude) would imply that factors  
147 other than wing color patterns, such as behavior or metabolism, explain adaptation to colder  
148 highland habitats in Ithomiini.

149

150

## 151 **Results**

152

153 To assess the thermal adaptation of Ithomiini butterflies, we examined the thermal and optical  
154 properties of the wings of 42 species in relation to climatic conditions. Unless specified otherwise,  
155 all statistical tests implemented Bayesian mixed models with Markov Chain Monte Carlo correcting  
156 for phylogenetic relatedness, with an associated Bayesian posterior P-value set to 0.05.

### 157 **Wing optical and thermal properties**

158 We first tested whether optical properties in the NIR wavelengths were correlated with those  
159 properties in the UV-Visible range, and whether those properties differed between transparent and  
160 opaque species, as defined hereafter. We measured transmission and reflection spectra on a 5mm-  
161 diameter spot on one hindwing and one forewing for each specimen, spanning the UV-Visible (300-  
162 700 nm) and NIR (700-2500 nm). We used the physical principle stating that Transmission ( $\lambda$ ) +  
163 Reflection ( $\lambda$ ) + Absorption ( $\lambda$ ) = 1 to compute the total absorption spectra over 300-2500 nm (Fig.  
164 4C). The transmission of the patch in the UV-Visible range was set as a measure for the degree of  
165 optical transparency. We split the species in two categories: transparent, for which wing  
166 transmission was higher than 35%, and opaque for the others (Table S1, Fig.S1).

167 Overall, UV-Visible transmission (300-700 nm), i.e., transparency as perceivable by  
168 butterflies and predators, was a good predictor of both overall absorption (300-2500 nm) and NIR  
169 absorption (700-2500 nm, Table S2, Fig. 1). NIR and UV-Visible absorption were highly correlated  
170 (Table S2, Fig. 1), be the species transparent or opaque. More transparent patches absorbed less  
171 light than opaque patches whatever the wavelength considered, supporting the *thermal cost*  
172 scenario for transparency (Fig. S2).

173 To investigate the thermal capacities of transparent wings and test whether they differ from  
174 those of opaque wings, we heated up wings with a flash illumination, and imaged them with an  
175 infrared camera to record temperature across the wing and its variation through time (Fig. 4A-B).  
176 Image analysis showed that the average heating capacity of the wing spot, represented by excess  
177 temperature  $\Delta T$  (maximum temperature reached after illumination - initial temperature), was closely  
178 related to its transparency, as estimated by the transmission in the UV-Visible range (Table S3,  
179 Fig. 2). Hence, the more transparent the spot, the less it heated up, in agreement with the *thermal*  
180 *cost* scenario.  $\Delta T$  of wing spots was also positively predicted by the mean total absorption of the  
181 spot and by its NIR absorption (Table S3, Fig. 2). Therefore, wings that absorbed more in the UV-  
182 Visible-NIR range or in the NIR range heated up more. In an in-depth exploration of the intra-wing  
183 variation in heating capacity, we extracted  $\Delta T$  on various points on different parts of the wings  
184 (veins and cells, i.e., the parts between veins), either in darkly colored patches DP (black to brown  
185 colors), lightly colored patches LP (for opaque species only, yellow to orange colors), or transparent  
186 patches TP, and on light LV or dark veins DV. A close look at the different areas and structures of  
187 the wings revealed that dark patches heated up significantly more than any other coloration on the  
188 wings, transparent or light (DP>(LP,TP) in Table S4, Fig. S3). Moreover, light patches heated up  
189 significantly more than transparent patches (LP>TP in Table S5, Fig. S3). Dark patches heated up  
190 more than dark veins (DP>DV in Table S6, Fig. S3), but on the other hand, light veins absorbed  
191 more heat than light patches (LV>LP in Table S7, Fig. S3). In all cases, the position of the patch  
192 with respect to the thorax, proximal or distal, played a role in predicting  $\Delta T$ , but this varied according  
193 to the color of the patch considered, showing no clear-cut trend (Table S4-7).

#### 194 **Wing trait distribution along climatic gradients**

195 We tested whether climatic variables predicted the proportion of dark patches on the wings of all  
196 the species, as posited by the TMH. We extracted 19 published average climatic variables for each  
197 species (29) that included temperature and precipitation descriptors and performed a PCA. PC1  
198 and PC2 explained respectively 49 % and 27.1 % of the total variation. Higher PC1 values  
199 corresponded to warmer climates, while higher PC2 values corresponded mainly to wetter and  
200 more time-stable climates (tables S8, S9, Fig. S4). Pearson's product-moment correlation tests  
201 showed that PC1 was strongly negatively correlated with altitude ( $R=-0.95$ ,  $N=42$ ,  $p < .0001$ ),  
202 meaning that species inhabiting higher altitude habitats had a lower PC1 value. PC2 did not  
203 correlate with altitude ( $R=0.24$ ,  $N=42$ ,  $p=0.12$ ). To test if opaque and transparent species had  
204 similar climatic ranges we used the Levene's heteroscedasticity test on climatic variables. We found  
205 that opaque species were restricted to warmer environments, while transparent species were  
206 ubiquitous and not associated to particular altitudes ( $F = 110.71$ ,  $p < .005$ ) (transparent species:  
207 mean=-0.27, var=10.56, opaque species: mean=1.08, var=1.09), in contradiction with the TMH.  
208 Opaque and transparent species did not significantly differ in their variance for PC2 ( $F=1.76$ ,



209  $p=0.19$ ) (transparent species: mean=0.29, var= 3.88, opaque species: mean=-1.89, var=3.45),  
210 showing that they did not segregate according to humidity or environmental stability gradients.  
211 Overall, climate did not predict wing optical properties. The degree of transmission of the wing spots  
212 over the range UV-Visible were not predicted by PC1, with a negligible positive effect for PC2 which  
213 goes against Gloger's rule (Table S10, Fig. S5). There was no significant association of spot  
214 absorption in the UV-Visible-NIR (table S11) or NIR ranges (table S12) with PC1 or PC2. By  
215 contrast, the average  $\Delta T$  of the whole wing surfaces was positively correlated to PC1 (Table S13,  
216 Fig. 3). In other words, species living in warm environments heated up more than butterflies living  
217 in colder environments.

218 Across all species, the proportion of dark surface on the wings increased with PC1 and  
219 was therefore higher in warmer environments (Table S14, Fig. S6). We found a similar trend when  
220 restricting the analysis to only transparent species (Table S15, Fig. S7). We examined whether this  
221 proportion varied with climate within the proximal zones alone, because wing conduction could be  
222 limited, and a patch was expected to have a greater thermal effect when closer to the body. Again,  
223 the proportion of dark surface in the proximal zones increased with PC1 (Table S16, Fig. S8), and  
224 was therefore higher in warmer environments, in contradiction with the TMH. The proportion of dark  
225 surface did not correlate with PC2, except when considering only proximal zones, indicating that  
226 proximally darker wings were associated with more humid habitats. Finally, we found no effect of  
227 climatic variables on total wing area, a proxy for butterfly size (Table S17).

228  
229

## 230 Discussion

231

### 232 Thermal properties correlate with optical properties in clearwing butterflies

233 The thermal imaging of *Ithomiini* wings reveals that opaque wings are on average more efficient to  
234 heat up than transparent wings. Hence, transparency entails thermal costs, a conclusion supported  
235 by the close-up study of the different wing patches, in agreement with the *thermal cost* scenario.  
236 The darker the color, the more the patch heats up. Therefore, transparent patches contribute little  
237 to wing heat absorption, in line with the long studied link between melanization and heating  
238 capacities (31). Consistent with this finding, the optical examination of the transparent wing spots  
239 reveals that the low absorption in the UV-Visible wavelength range is not compensated by a higher  
240 absorption in the invisible NIR range, and therefore wing transparency comes at the cost of light  
241 absorption. This result departs from findings in other organisms where visible reflectance tends to  
242 be a poor predictor of NIR reflectance (32). Moreover, transparent spots always absorb less light  
243 than opaque ones, regardless of the wavelength considered. This is in agreement with the  
244 correlation of the UV-Visible and NIR spectra that has been previously described for transmission



245 (21) or reflection (18, 19) in interspecific studies of butterflies taxa. Yet, veins in transparent  
246 Ithomiini species are always covered with melanized scales. Those veins heat up significantly more  
247 than transparent and even lightly colored patches, and likely represent a major part of the overall  
248 wing thermal capacities by providing heat to the dynamic hemolymph flow system to the thorax  
249 (33).

250 In Ithomiini, absorption decreases in long wavelengths, and is quite low in the NIR for all  
251 the studied species. An interspecific comparison of the absorption of longer wavelengths (~8-12  
252  $\mu\text{m}$ ), especially infrared radiated by the environment, remains to be carried out as this wavelength  
253 range is supposed to have greater thermal impact. However, the thermal imaging results clearly  
254 show that transparent patches are poorer at accumulating heat than opaque patches, suggesting  
255 an absence of compensation in the far infrared range.

### 256 **The altitudinal distribution of transparent species contradicts the thermal melanism** 257 **hypothesis**

258 This study confirms the counterintuitive altitudinal distribution of Ithomiini wing patterns (30). While  
259 the opaque species are only found in warm climates, clearwing species are ubiquitous and widely  
260 distributed, from hot lowlands to the cold Andean highlands. Moreover, among clearwing species,  
261 the proportion of opaque patches on the wings decreases in colder environments, i.e. at higher  
262 altitudes, challenging the long history of studies supporting the TMH in butterflies and insects  
263 e.g.(15, 16, 34, 35), but adding to the observation that TMH does not apply to all taxa or  
264 communities. For instance a recent study found support for TMH in geometrids but not in noctuids  
265 found in the same study sites (36). Yet, these studies often focus on temperate climates.  
266 Neotropical case studies are scarce and show mixed support to the TMH. Two closely related  
267 neotropical butterfly genera, *Catastica* and *Leptophobia* have a divergent coloration distribution  
268 along altitudinal gradients (37), possibly explained by different behaviors and elevation ranges.  
269 While body and wing colorations become darker with increasing altitude in *Catastica*, *Leptophobia*  
270 shows a reversed pattern, similar to that observed in Ithomiini. In the case of Ithomiini, not only the  
271 non-conformity to TMH is outstanding, but there is no high NIR absorbance to compensate the poor  
272 UV-Visible absorption that would make highland butterflies more adapted to cooler conditions.

273 The NIR range is expected to be only subjected to thermoregulatory pressures, unlike UV-  
274 Visible wavelengths involved in vision. Indeed, NIR reflection spectra of Australian and European  
275 butterflies communities are well predicted by climatic conditions (18, 19). In contrast to their  
276 conclusions, our study of the absorption properties of wing spots showed that in general, climatic  
277 conditions do not predict wing absorption in any radiation range. Moreover, the exploration of wing  
278 heating capacities shows that Ithomiini species living in colder environments are less efficient to  
279 heat up than species living in warmer climates, adding even more to the thermal cost of

280 transparency. Finally, there is hardly any link between thermal or optical properties and humidity,  
281 and as such this study does not support Gloger's rule in Ithomiini.

282         Adaptation to cooler conditions is not the only thermal constraint faced by organisms, as  
283 high temperature may also be challenging. Here we found that opaque species, which absorb more  
284 radiation and have higher thermal capacities, live in environments where they are most exposed to  
285 heat. For ectotherms, avoiding overheating (i.e. increasing body temperature above a critical  
286 temperature threshold) can be challenging. Butterflies may have physiological adaptations (38) or  
287 behavioral adjustments, such as changing the position of their wings according to environmental  
288 radiations (33). Information on the metabolism and behavior of Ithomiini *in natura* would shed light  
289 on their altitudinal adaptation, but are currently lacking. In addition, microhabitat variability can  
290 result in individuals sharing the same overall environment being exposed to contrasting light and  
291 temperature conditions. Microhabitat preferences thus likely play a role in adjusting body  
292 temperature (38, 39). However, in lowland ithomiine communities, butterflies with transparent wing  
293 patterns mostly fly in the understory, close to the vegetation and out of direct sunlight, while the  
294 proportion of species with opaque wings increases with height in the canopy (40). The latter are  
295 therefore more exposed to solar radiation, another counterintuitive distribution in relationship to  
296 thermoregulation.

#### 297 **Transparency under multiple selection pressures**

298 Colorations in butterflies, and therefore wing optical properties, are under multiple selection  
299 pressures as they are involved in anti-predator defenses, signaling to conspecifics and thermal  
300 adaptation, with potential trade-offs (9). Consequently, selection for crypsis and aposematism could  
301 be detrimental for thermal capacities (41). Wood tiger moths are a good example of the  
302 phenomenon: larvae with large black patches are at a thermal advantage compared to larvae with  
303 equally black and orange patches, but the latter display a more efficient aposematic signal (42).  
304 Imagoes display latitudinal variation in wing pattern, consistent with the TMH, which incurs cost in  
305 the efficiency of warning signals as melanic individuals experience more predation (34). In Ithomiini,  
306 the existence and pervasiveness of transparency is surprising given that those butterflies are toxic  
307 and harbor aposematic signals. Previous work has shown that transparency in Ithomiini reduces  
308 detection and attacks by naïve predators (27). Even though transparent patches are likely part of  
309 the aposematic signal (22), transparency may reduce predator learning speed and memorization  
310 of prey, as indirectly suggested by the observation that unpalatability tends to be stronger in  
311 clearwing than in opaque species (43). Thus, transparency may incur a cost on aposematism, with  
312 a trade-off between crypsis and aposematism. A possible explanation for the unexpected altitudinal  
313 distribution of transparency in Ithomiini species may be different predation pressures at different  
314 altitudes in tropical mountains (44), which may favor crypsis over aposematism at higher altitudes,  
315 as observed in Andean arctiine moths or which conspicuousness decreases with height (45).

316 Therefore, the altitudinal distribution of color patterns in ithomiine may be primarily driven by  
317 predation rather than climatic conditions.

### 318 **Conclusion**

319 In Ithomiini, the altitudinal distribution of wing patterns is unlikely driven by thermal constraints, and  
320 goes against the predictions of the thermal melanism hypothesis. Transparent wings have a low  
321 absorption of wavelengths in the UV-Visible-NIR range and this comes at a cost regarding heating  
322 capacities. Conversely, transparency in these butterflies has probably evolved in response to  
323 selection incurred by predation. The results question the critical significance of wing color pattern  
324 for thermal adaptation in tropical ectotherms and lead the way to further investigations about  
325 metabolic and behavioral thermoregulation, and their relative contributions to climatic adaptation in  
326 these species.

327

328

### 329 **Materials and Methods**

330

#### 331 **Specimen sampling, climatic data and phylogeny**

332 We studied wings of dried Ithomiini butterfly specimens, preserved in glassine envelopes, collected  
333 between 2005 and 2018 in south America. We focused on 42 species represented by two or more  
334 females to reduce the potential variance due to sexual differences (Table S1). Measurements were  
335 taken on one hindwing and one forewing of each specimen. The selected species spanned a large  
336 range of wing coloration, from fully opaque to highly transparent, and are evenly distributed along  
337 the altitudinal gradient and across the phylogeny. GPS data on species distributions were obtained  
338 from a database that contains more than 3500 occurrences of specimens of the species studied  
339 here (29). We extracted the corresponding 19 climate variables (Table S8-9., Fig. S4) from  
340 WorldClim2 historical climatic data (46) with a resolution of 2.5 arc-minutes. Variables were  
341 averaged for each species. For the phylogenetic comparative analyses, we used the most  
342 comprehensive phylogeny of the Ithomiini to date (28), which comprises 340 out of 393 extant taxa.

#### 343 **Spectrophotometry measurements**

344 To quantify the extent to which wings transmit and absorb light, we performed spectrophotometry  
345 measurements on a spot of 5 mm of diameter on the hindwing and forewing of each specimen. For  
346 transparent species, the spot was in the proximal transparent patch. For opaque species, the spot  
347 was located on the center of the proximal zone of the wing. Since a wing can reflect and transmit  
348 a large proportion of the incident light, we measured both total (specular + diffuse) reflection and  
349 total (specular + diffuse) transmission spectra of each patch, with an Agilent CARY 5000 UV-  
350 Visible-NIR spectrophotometer, equipped with an integrating sphere, over the range 300-2500 nm,  
351 which includes ultraviolet (UV), Visible, and near-infrared (NIR) wavelengths. Wings were

352 maintained in a black paper mask with an opening of 5 mm of diameter. Spectra were measured  
353 relative to a dark (paper mask without the wings, light off) and to a white reference (Spectralon  
354 white diffuse reflectance standard), with the paper mask for reflection, nothing for transmission,  
355 light on. The resulting total absorption spectra were calculated for each wavelength  $\lambda$  as Absorption  
356 ( $\lambda$ ) = 1 - (Transmission ( $\lambda$ ) + Reflection ( $\lambda$ )) according to the law of conservation of energy (Fig. 4).  
357 The negative values due to the noise of the signal were fixed to zero with the function `fixneg` of the  
358 package `Pavo` in R (47), and each spectrum was smoothed with the `loess` function in R. We  
359 quantified mean absorption at different wavelength ranges, in the UV-Visible between 300-700 nm,  
360 in the NIR between 700-2500 nm, and the total 300-2500 nm. Mean transmission in the UV-Visible  
361 range 300-700 nm was measured as a proxy for animal-visible transparency. We divided the  
362 species into two categories, transparent and opaque, based on a threshold of mean transmission  
363 at 35% in the UV-Visible, matching butterflies and predators' visual perception (Table S16).

#### 364 **Thermal measurements**

365 To characterize and compare the wing thermal characteristics, we measured wing temperature  
366 kinetics following instant exposure to a flash light (Fig. 4B). We conducted stimulated heating  
367 measurements on one hindwing and one forewing for each specimen, with a Neewer professional  
368 photo system flash lamp N-300W set at maximum power, which emits over the UV-Visible-IR range.  
369 Wings were recorded by an infrared camera T650sc 2019 FLIR Systems equipped with a FLIR lens  
370 T197-915. Emissivity was set at 0.95. Wings were kept at a constant ambient temperature of 23°C  
371 prior to the experiment. We placed each single wing horizontally on a custom grid made of 3 human  
372 hair in a frame to minimize contact with any surface, 6 cm below the camera and the flash and 30  
373 cm above a table covered with white paper, to avoid background interference with the measure.  
374 The flash lasted for 1/800 seconds. We started the recording a few seconds before activating the  
375 flash, and let the record run for 10 seconds. Each movie was recorded at 30 images.second<sup>-1</sup>. From  
376 the movies, we extracted the thermal kinetics - temperature as a function of time - of different  
377 regions of interest on the wings with FLIR ResearchIR Max software, and more specifically the  
378 excess temperature  $\Delta T$  as the difference between the maximal temperature attained by the region  
379 of interest after the flash hits minus the temperature prior to the flash. We extracted mean  $\Delta T$  of  
380 the overall wing surface, mean  $\Delta T$  of the spot measured in spectrophotometry and finally  $\Delta T$  of  
381 precise points of interest on each wings as follows: 6 points in the dark colored patches DP (black  
382 to brown colors), 6 points in light colored patches LP (yellow to orange colors and for opaque  
383 species only), 6 points in the transparent patches TP (for transparent species only), and 8 points  
384 on veins, assigned to a category depending on their color: dark veins DV (black to brown) and light  
385 veins LV (yellow to orange).

386 **Image analysis**

387 We used digital photography to quantify the proportion of dark pigmented surface on the full wings  
388 of all the specimens. Melanization in proximal zones of the wing can be of primary importance in  
389 thermoregulation as the zone is closer to the thoracic muscles (8). We also quantified the color  
390 proportion separately on the proximal and distal zone of each wing. We set the limit between the  
391 zones as the perpendicular line to the middle of the transect line from the wing insertion to its apex.  
392 We cropped the photos for each zone considered and the background was filled with green, a color  
393 ignored when calculating the color proportions. In R, we used the `getKMeanColors` function from  
394 `colordistance` package (48) to sort the pixels in clusters according to their RGB values. We set the  
395 number of clusters to two, corresponding to mainly dark and brown, versus transparent, or any  
396 other light colors in opaque wings. With ImageJ 1.52 (49) we computed the total surface of each  
397 wing in mm<sup>2</sup>.

398 **Statistical analyses**

399 We explored various scenarios linking absorption, transmission, thermal capacities and climatic  
400 variables across the 42 species of the dataset (see supplementary materials for model details and  
401 results). Because specimens are not independent and the species are related through the  
402 phylogeny, we implemented for each test Bayesian mixed models with Markov Chain Monte Carlo,  
403 correcting for phylogenetic relatedness, using the R package `MCMCglmm` (50) and the phylogeny  
404 from (28). We controlled for chain convergence visually and with the Heidelberg stationarity test  
405 diagnostic function of convergence `heidel.diag` from the R package `coda` (51). To get accurate  
406 estimations of posterior distributions and avoid chain autocorrelation, we adjusted the iterations,  
407 burn-in and thinning for each model to ensure an effective sample size across all parameters of at  
408 least 1000. Models were run with a weakly informative prior for random effect and residual  
409 variances ( $V = 1$ ,  $\nu = 0.002$ ) not to constrain the exploration of parameter values. We selected the  
410 best model with a backward selection of fixed parameters based on Bayesian P-value of 0.05,  
411 within the 95% confidence interval excluding zero. In all the models, species identity was  
412 implemented as a random factor. We included all individuals in the models unless specified  
413 otherwise.

414  
415  
416  
417  
418  
419  
420

421 **Acknowledgments**

422

423 This work was funded by Clearwing ANR project (ANR-16-CE02-0012), HFSP project on  
424 transparency (RGP0014/2016). VO is recipient of a doctoral fellowship from the doctoral school  
425 FIRE, Learning Planet Institute. We are strongly grateful to authorities in Peru and Ecuador for  
426 providing collecting permits (Ecuador: 005-IC-FAU-DNBAPVS/MA, 019-IC-FAU-  
427 DNBAPVS/MA021; Peru: 236-2012-AG-DGFFS-DGEFFS, 201-2013-MINAGRI-DGFFS/DGEFFS,  
428 002-2015-SERFOR-DGGSPFFS, 373-2017-SERFOR-DGGSPFFS; Gobierno Regional San  
429 Martín PEHCBM: 124-2016-GRSM/PEHCBM-DMA/EII-ANP/JARR). We warmly thank Raúl Aldaz,  
430 Paula Santacruz and Alexandre Toporov for providing help in the field, and Santiago Villamarin,  
431 the Museo de Historia Natural and Professor Gerardo Lamas for their support. We also thank Jean-  
432 Luc Bodnar and Kamel Mouhoubi from Reims University for technical advice with IR imaging, Pierre  
433 de Villemereuil for his help with Bayesian analysis, Maël Doré for bioclimatic and distribution data  
434 sharing, Willy Daney de Marcillac for his advice with optical measurements and Serge Berthier for  
435 inspiring discussion on clearwing butterflies.

436

437 **References**

438

- 439 1. D. G. Stavenga, H. L. Leertouwer, B. D. Wilts, Coloration principles of nymphaline  
440 butterflies - thin films, melanin, ommochromes and wing scale stacking. *Journal of*  
441 *Experimental Biology* **217**, 2171–2180 (2014).
- 442 2. S. Berthier, *Iridescences: the physical colors of insects.*, Springer, Berlin, Germany. (2007).
- 443 3. H. Tada, S. E. Mann, I. N. Miaoulis, P. Y. Wong, Microscale Radiative Effects in Complex  
444 Microstructures of Iridescent Butterfly Wing Scales. *MRS Proc.* **489**, 173 (1997).
- 445 4. D. J. Kemp, Female butterflies prefer males bearing bright iridescent ornamentation. *Proc.*  
446 *R. Soc. B* **274**, 1043–1047 (2007).
- 447 5. J. A. Endler, Progressive background in moths, and a quantitative measure of crypsis.  
448 *Biological Journal of the Linnean Society* **22**, 187–231 (1984).
- 449 6. J. Skelhorn, H. M. Rowland, M. P. Speed, G. D. Ruxton, Masquerade: Camouflage Without  
450 Crypsis. *Science* **327**, 51–51 (2010).
- 451 7. E. B. Poulton, The Experimental Proof of the Protective Value of Colour and Markings in  
452 Insects in reference to their Vertebrate Encmies. *Proceedings of the Zoological Society of*  
453 *London* **55**, 191–274 (1887).



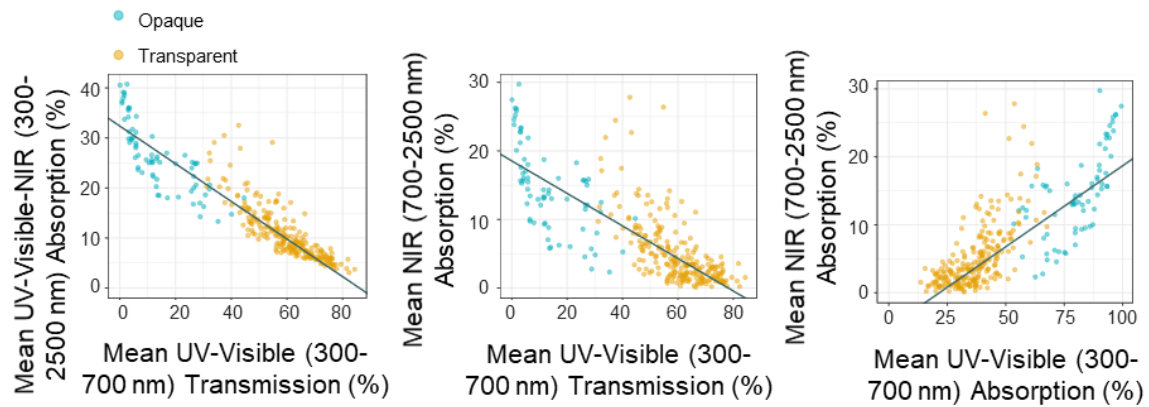
- 454 8. L. T. Wasserthal, The rôle of butterfly wings in regulation of body temperature. *Journal of*  
455 *Insect Physiology* **21**, 1921–1930 (1975).
- 456 9. E. G. Postema, M. K. Lippey, T. Armstrong-Ingram, Color under pressure: how multiple  
457 factors shape defensive coloration. *Behavioral Ecology*, arXiv:2205.05666 (2022).
- 458 10. B. Heinrich, “Mechanisms of Insect Thermoregulation” in *Effects of Temperature on*  
459 *Ectothermic Organisms*, W. Wieser, Ed. (Springer Berlin Heidelberg, 1973), pp. 139–150.
- 460 11. J. Eilers, C. L. Boggs, Functional ecological implications of intraspecific differences in wing  
461 melanization in *Colias* butterflies: WING DARKNESS, FLIGHT AND EGG MATURATION.  
462 *Biological Journal of the Linnean Society* **82**, 79–87 (2004).
- 463 12. J. Roland, Melanism and diel activity of alpine *Colias* (Lepidoptera: Pieridae). *Oecologia* **53**,  
464 214–221 (1982).
- 465 13. S. Clusella Trullas, J. H. van Wyk, J. R. Spotila, Thermal melanism in ectotherms. *Journal of*  
466 *Thermal Biology* **32**, 235–245 (2007).
- 467 14. S. Clusella-Trullas, J. S. Terblanche, T. M. Blackburn, S. L. Chown, Testing the thermal  
468 melanism hypothesis: a macrophysiological approach. *Funct Ecology* **22**, 232–238 (2008).
- 469 15. C. S. Guppy, The adaptive significance of alpine melanism in the butterfly *Parnassius*  
470 *phoebus* F. (Lepidoptera: Papilionidae). *Oecologia* **70**, 205–213 (1986).
- 471 16. D. Zeuss, R. Brandl, M. Brändle, C. Rahbek, S. Brunzel, Global warming favours light-  
472 coloured insects in Europe. *Nat Commun* **5**, 3874 (2014).
- 473 17. D. Stuart-Fox, E. Newton, S. Clusella-Trullas, Thermal consequences of colour and near-  
474 infrared reflectance. *Phil. Trans. R. Soc. B* **372**, 20160345 (2017).
- 475 18. C. Kang, *et al.*, Climate predicts both visible and near-infrared reflectance in butterflies.  
476 *Ecology Letters* **24**, 1869–1879 (2021).
- 477 19. J. T. Munro, *et al.*, Climate is a strong predictor of near-infrared reflectance but a poor  
478 predictor of colour in butterflies. *Proc. R. Soc. B* **286**, 20190234 (2019).
- 479 20. K. Delhey, J. Dale, M. Valcu, B. Kempenaers, Reconciling ecogeographical rules: rainfall and  
480 temperature predict global colour variation in the largest bird radiation. *Ecol Lett* **22**, 726–  
481 736 (2019).
- 482 21. D. Gomez, *et al.*, Wing transparency in butterflies and moths: structural diversity, optical  
483 properties, and ecological relevance. *Ecol Monogr* **91** (2021).
- 484 22. C. S. Pinna, *et al.*, Mimicry can drive convergence in structural and light transmission  
485 features of transparent wings in Lepidoptera. *eLife* **10**, e69080 (2021).



- 486 23. A. F. Pomerantz, *et al.*, Developmental, cellular, and biochemical basis of transparency in  
487 clearwing butterflies. *Journal of Experimental Biology*, jeb.237917 (2021).
- 488 24. R. H. Siddique, G. Gomard, H. Hölscher, The role of random nanostructures for the  
489 omnidirectional anti-reflection properties of the glasswing butterfly. *Nat Commun* **6**, 6909  
490 (2015).
- 491 25. M. Arias, *et al.*, Partial wing transparency works better when disrupting wing edges:  
492 Evidence from a field experiment. *Journal of Evolutionary Biology* **34**, 1840–1846 (2021).
- 493 26. M. Arias, M. Elias, C. Andraud, S. Berthier, D. Gomez, Transparency improves concealment  
494 in cryptically coloured moths. *J Evol Biol* **33**, 247–252 (2020).
- 495 27. M. Arias, *et al.*, Transparency reduces predator detection in mimetic clearwing butterflies.  
496 *Funct Ecol* **33**, 1110–1119 (2019).
- 497 28. N. Chazot, *et al.*, Renewed diversification following Miocene landscape turnover in a  
498 Neotropical butterfly radiation. *Global Ecol Biogeogr*, geb.12919 (2019).
- 499 29. M. Doré, *et al.*, Anthropogenic pressures coincide with Neotropical biodiversity hotspots in  
500 a flagship butterfly group. *Diversity and Distributions* **28**, 2912–2930 (2022).
- 501 30. N. Chazot, *et al.*, Mutualistic Mimicry and Filtering by Altitude Shape the Structure of  
502 Andean Butterfly Communities. *The American Naturalist* **183**, 26–39 (2014).
- 503 31. H. Schmitz, Thermal characterization of butterfly wings—1. Absorption in relation to  
504 different color, surface structure and basking type. *Journal of Thermal Biology* **19**, 403–412  
505 (1994).
- 506 32. K. Nussear, E. Simandle, R. Tracy, Misconceptions about colour, infrared radiation, and  
507 energy exchange between animals and their environments. *Herpetological Journal* **10**,  
508 119–122 (2000).
- 509 33. C.-C. Tsai, *et al.*, Physical and behavioral adaptations to prevent overheating of the living  
510 wings of butterflies. *Nat Commun* **11**, 551 (2020).
- 511 34. R. H. Hegna, O. Nokelainen, J. R. Hegna, J. Mappes, To quiver or to shiver: increased  
512 melanization benefits thermoregulation, but reduces warning signal efficacy in the wood  
513 tiger moth. *Proc. R. Soc. B* **280**, 20122812 (2013).
- 514 35. J. Roland, Effect of melanism of alpine *Colibris nastes* butterflies (Lepidoptera: Pieridae) on  
515 activity and predation. *Can Entomol* **138**, 52–58 (2006).
- 516 36. L. Heidrich, *et al.*, Noctuid and geometrid moth assemblages show divergent elevational  
517 gradients in body size and color lightness. *Ecography* **44**, 1169–1179 (2021).
- 518 37. P. C. Dufour, *et al.*, Divergent melanism strategies in Andean butterfly communities  
519 structure diversity patterns and climate responses. *J Biogeogr* **45**, 2471–2482 (2018).

- 520 38. G. Montejo-Kovacevich, *et al.*, Microclimate buffering and thermal tolerance across  
521 elevations in a tropical butterfly. *Journal of Experimental Biology*, jeb.220426 (2020).
- 522 39. I. Kleckova, M. Konvicka, J. Klecka, Thermoregulation and microhabitat use in mountain  
523 butterflies of the genus *Erebia*: Importance of fine-scale habitat heterogeneity. *Journal of*  
524 *Thermal Biology* **41**, 50–58 (2014).
- 525 40. K. R. Willmott, J. C. Robinson Willmott, M. Elias, C. D. Jiggins, Maintaining mimicry  
526 diversity: optimal warning colour patterns differ among microhabitats in Amazonian  
527 clearwing butterflies. *Proc. R. Soc. B* **284**, 20170744 (2017).
- 528 41. L. Heidrich, *et al.*, The dark side of Lepidoptera: Colour lightness of geometrid moths  
529 decreases with increasing latitude. *Global Ecol Biogeogr* **27**, 407–416 (2018).
- 530 42. C. Lindstedt, L. Lindström, J. Mappes, THERMOREGULATION CONSTRAINS EFFECTIVE  
531 WARNING SIGNAL EXPRESSION. *Evolution* **63**, 469–478 (2009).
- 532 43. M. McClure, *et al.*, Why has transparency evolved in aposematic butterflies? Insights from  
533 the largest radiation of aposematic butterflies, the Ithomiini. *Proc. R. Soc. B* **286**, 20182769  
534 (2019).
- 535 44. T. Roslin, *et al.*, Higher predation risk for insect prey at low latitudes and elevations.  
536 *Science* **356**, 742–744 (2017).
- 537 45. K. Fiedler, G. Brehm, Aposematic Coloration of Moths Decreases Strongly along an  
538 Elevational Gradient in the Andes. *Insects* **12**, 903 (2021).
- 539 46. S. E. Fick, R. J. Hijmans, WorldClim 2: new 1-km spatial resolution climate surfaces for  
540 global land areas. *International Journal of Climatology* **37**, 4302–4315 (2017).
- 541 47. R. Maia, C. M. Eliason, P.-P. Bitton, S. M. Doucet, M. D. Shawkey, pavo : an R package for  
542 the analysis, visualization and organization of spectral data. *Methods Ecol Evol*, n/a-n/a  
543 (2013).
- 544 48. H. I. Weller, M. W. Westneat, Quantitative color profiling of digital images with earth  
545 mover’s distance using the R package colordistance. *PeerJ* **7**, e6398 (2019).
- 546 49. J. Schindelin, *et al.*, Fiji: an open-source platform for biological-image analysis. *Nature*  
547 *Methods* **9**, 676–682 (2012).
- 548 50. J. D. Hadfield, MCMC Methods for Multi-Response Generalized Linear Mixed Models: The  
549 **MCMCglmm** R Package. *J. Stat. Soft.* **33** (2010).
- 550 51. M. Plummer, N. Best, K. Cowles, K. Vines, “CODA: Convergence Diagnosis and Output  
551 Analysis for MCMC” in R News, (2006), pp. 7–11.

552  
553  
554  
555  
556  
557  
558  
559  
560  
561  
562  
563  
564  
565  
566  
567  
568  
569  
570  
571  
572  
573  
574  
575  
576  
577  
578  
579  
580  
581  
582  
583  
584  
585  
586  
587



588

589 **Figure 1.** Relationship between absorption and transmission spectra at different ranges: overall  
590 UV-Visible-NIR (300-2500 nm) absorption against UV-Visible (300-700 nm) transmission, NIR  
591 (700-2500 nm) absorption against UV-Visible transmission, NIR (700-2500 nm) absorption  
592 against UV-Visible (300-700 nm) absorption. All relationships are significant and the solid line is  
593 drawn from the prediction of the Bayesian phylogenetic mixed model (see Table S2) (N opaque =  
594 72, N transparent = 235).

595

596

597

598

599

600

601

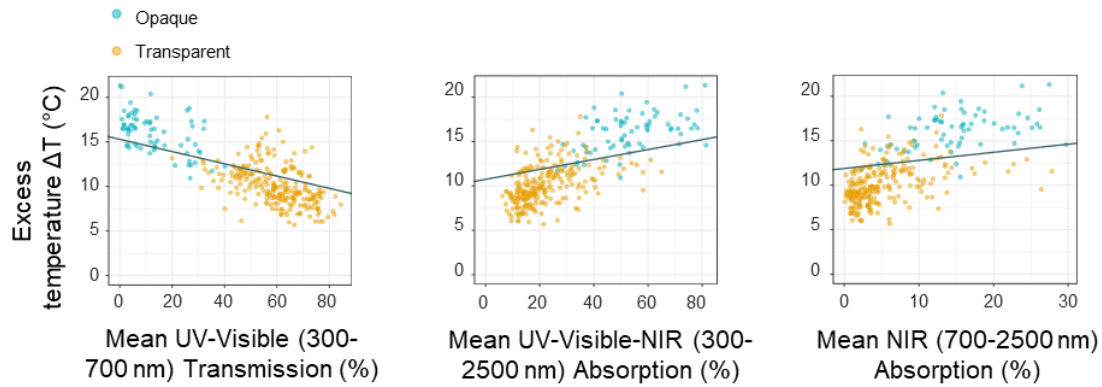
602

603

604

605

606



607

608 **Figure 2.** The thermal properties of wing spots represented by the Excess Temperature  $\Delta T$   
609 ( $T^{\circ}\text{final} - T^{\circ}\text{initial}$ ) under a flash illumination, extracted from the thermal imaging, against their  
610 optical properties at different ranges: UV-Visible (300-700 nm) transmission, UV-Visible-NIR (300-  
611 2500 nm) absorption, and NIR (700-2500 nm) absorption. All relationships are significant and the  
612 solid line is drawn from the prediction of the Bayesian phylogenetic mixed model (see Table S3) (N  
613 opaque = 72, N transparent = 235).

614

615

616

617

618

619

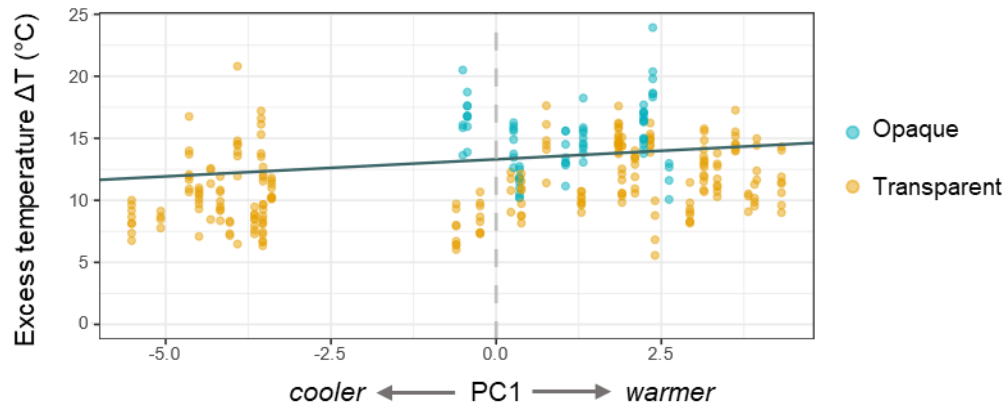
620

621

622

623

624



625

626 **Figure 3.** Wings mean Excess Temperature  $\Delta T$  ( $T^{\circ}\text{final} - T^{\circ}\text{initial}$ ) under a flash illumination,  
627 extracted from the thermal imaging, as a function of climatic principal component PC1. The  
628 relationship is significant and the solid line is drawn from the prediction of the Bayesian phylogenetic  
629 mixed model (see Table S13) (N opaque = 72, N transparent = 235).

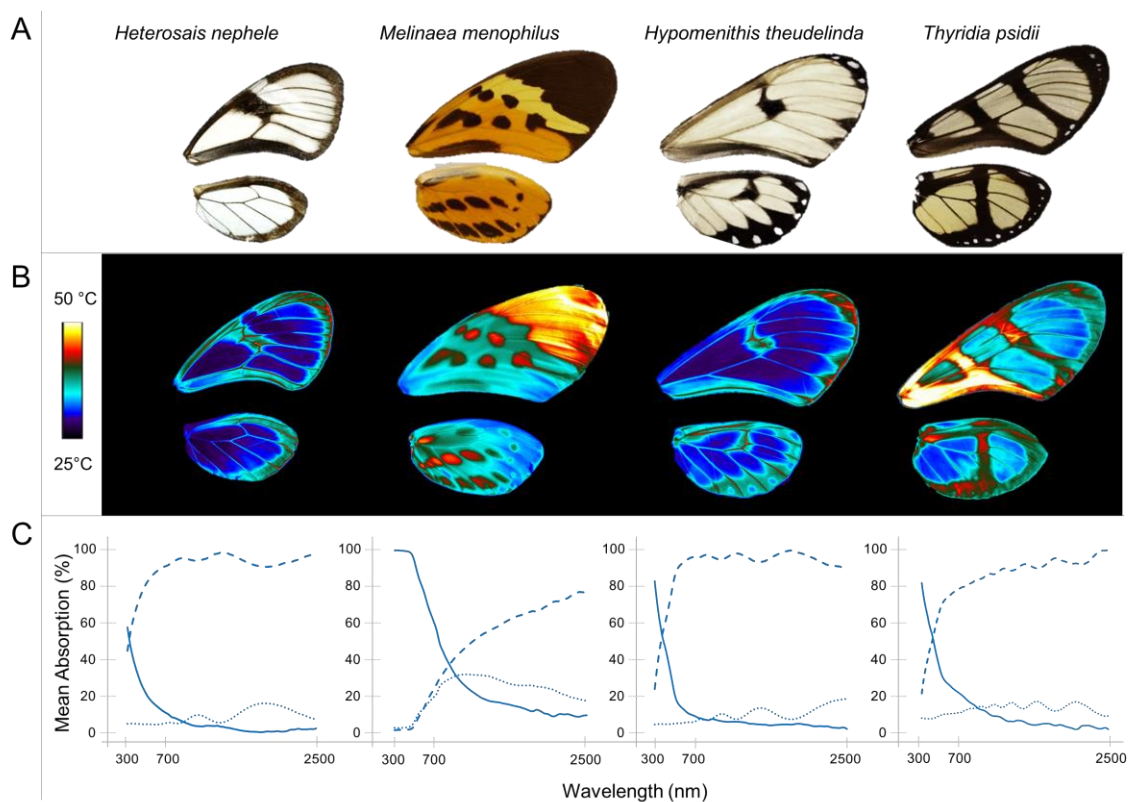
630

631

632

633

634



635

636 **Figure 4.** Examples of optical and thermal imaging on the wings of four species of different opacity.  
637 A: Photos under standard illumination of the hindwings and forewings of four of the species studied,  
638 *Heterosais nephele*, *Melinaea menophilus*, *Hypomenithis theudelinda*, *Thyridia psidii*. B:  
639 Visualization of the thermal imaging in false colors of the same wings under a flash light. C:  
640 Corresponding measured transmission (dashed lines) and reflection (dotted lines) spectra in  
641 percentage, for a spot of 5 mm of diameter on the proximal forewing of each butterfly, from 300 to  
642 2500 nm, and the resulting computed absorption spectra (solid lines) for each wavelength  $\lambda$  as  
643  $Absorption(\lambda) + Transmission(\lambda) + Reflection(\lambda) = 1$ .

644

645

646

647